

DOI: 10.1134/S0869864317060063

## **Viscous near-wall flow in a wake of circular cylinder at moderate Reynolds numbers<sup>\*</sup>**

**D.I. Okhotnikov<sup>1</sup>, V.M. Molochnikov<sup>2,3\*</sup>, A.B. Mazo<sup>1</sup>, A.V. Malyukov<sup>2</sup>,  
A.E. Goltzman<sup>2</sup>, and I.I. Saushin<sup>2</sup>**

<sup>1</sup>*Kazan Federal University, Kazan, Russia*

<sup>2</sup>*Kazan Scientific Center of RAS, Kazan, Russia*

<sup>3</sup>*Kazan National Research Technical University named after A.N. Tupolev, Kazan, Russia*

E-mail: vmolochnikov@mail.ru<sup>\*</sup>

*(Received January 19, 2017; in revised form February 28, 2017)*

Here we present the results of experimental investigation of a cross flow around a circular cylinder mounted near the wall of a channel with rectangular cross section. The experiments were carried out in the range of Reynolds numbers corresponding to the transition to turbulence in a wake of the cylinder. Flow visualization and SIV-measurements of instantaneous velocity fields were carried out. Evolution of the flow pattern behind the cylinder and formation of the regular vortex structures were analyzed. It is shown that in the case of flow around the cylinder, there is no spiral motion of fluid from the side walls of the channel towards its symmetry plane, typical of the flow around a spanwise rib located on the channel wall. The laminar-turbulent transition in the wake of the cylinder is caused by the shear layer instability.

**Key words:** circular cylinder, channel, visualization, SIV-measurements, separation region, shear layer, loss of stability, transition to turbulence, velocity profiles, root-mean-square velocity fluctuations.

### **Introduction**

Investigation of the cross flow of viscous fluid around a cylinder is one of the classical problems of mechanics. To date, it has been studied well [1]. It is known that in the range of Reynolds number  $Re_d \approx 60-5 \cdot 10^5$ , calculated by cylinder diameter  $d$  and freestream velocity  $U$ , the regular vortices (the Karman street) are periodically formed behind the cylinder. In the limits of this range, starting from  $Re_d \approx 10^3$ , the dimensionless vortex shedding frequency characterized by Strouhal number  $Sh$  remains practically unchanged, and for the unlimited external flow, it is  $Sh \approx 0.21$ .

The problem of viscous flow around a circular cylinder located near a wall has been studied less. However, this flow configuration is often met in various engineering applications: heat exchangers and cooling systems, pipelines for various purposes, etc. The main studies in this field deal with the dependence of vortex shedding frequency from the cylinder surface on dis-

<sup>\*</sup> The work was financially supported by the Russian Science Foundation (Project No. 16-19-10336).

tance  $\delta$  between the cylinder and wall (screen). For instance, in [2], this flow was simulated numerically by the method of discrete vortices. The authors concluded that the screen has a little effect on the frequency of vortex formation. A similar result was obtained in experiments of [3], where the flow around a cylinder near the wall at  $Re_d \approx 4.5 \cdot 10^4$  was studied. It was shown that at a change in gap  $\delta$ , frequency  $Sh$  remains almost constant. However, in some studies, the opposite conclusions were obtained. For example, pressure pulsations on the wall caused by a vortex street behind a transverse cylinder at  $Re_d \approx 10^5$  were measured in [4]. The results of measurements showed that the frequency of vortex formation in the Karman street is proportional to the distance between the cylinder and wall. The authors of [5] came to the same conclusion.

The flow structure in a wake of a circular cylinder transverse to the near-wall flow is studied even less. Thus, regularities of distribution of heat transfer and surface friction coefficients in the boundary layer on a plate with transversely streamlined cylinder were experimentally investigated in [6] at various distances between the cylinder and plate, and hydrodynamic and thermal flow patterns in the cylinder wake near the wall were studied in [7]. Experimental data on the velocity fields, distribution of streamwise component of surface friction, heat flux into the wall, and pressure pulsations on the wall in the cylinder wake were obtained by the authors of [8]. All these investigations were carried out for Reynolds numbers  $Re_d > 10^4$  corresponding to the turbulent flow in the boundary layer of the plate (wall) with a transversely streamlined cylinder nearby.

Thesis [9] deals with the detailed research of the effect of gap size  $\delta$  between the cylinder and wall on the flow around the cylinder at high (near-critical) Reynolds numbers. It is shown that with decreasing  $\delta$ , the lift force of the cylinder increases, and resistance varies little. At  $\delta < 0.15 d$ , the effect of screen becomes decisive: symmetry of the flow around the cylinder is violated, the frontal stagnation point shifts toward the screen, and position of separation points and sizes of rarefaction zones on the lateral parts of the cylinder surface change.

The flow around the circular cylinder located near the plane wall was investigated experimentally by PIV at  $Re_d = 8700$  in [10]. Three different flow regimes were detected depending on the size of a gap between the cylinder and wall. The authors concluded that at  $\delta > 0.8d$ , the vortex wake is almost symmetrical and the wall effect is insignificant. With a decrease in  $\delta$ , the vortex wake becomes discontinuous, small-scale vortex structures appear, and at gap  $\delta < 0.3d$ , the jet formed in the gap destroys the shear layer on the cylinder surface close to the wall and prevents the beginning of periodic vortex formation. PIV was also used in [11] to study the influence of gap size  $\delta$  on separation of the boundary layer on the wall, position of the separation point on the cylinder, and vortex shedding frequency  $Sh$ . Experiments were carried out with seven different relative gap sizes  $\delta/d$  from 0 to 2.0 at three  $Re_d$  values: 840, 4150, and 9500. It was shown that at  $\delta/d > 0.3$ , an increase in the gap leads to a very slow change in the wake flow pattern behind the cylinder. Four characteristic regimes of the flow around the cylinder near the wall were distinguished in [12] depending on the gap size. The first regime corresponds to  $\delta/d < 0.125$ , when the flow in the gap is completely suppressed or its velocity is small. The flow separates in front of the cylinder and behind it. In the second regime, at  $0.125 < \delta/d < 0.5$ , we can see pronounced merging of the near-wall shear layer behind the cylinder with the wall boundary layer. The third regime includes the flow with the relative gap of  $0.5 < \delta/d < 0.75$ . In this regime, the beginning of vortex shedding from the cylinder is observed. The fourth regime is characterized by the largest relative gap size:  $\delta/d > 1$ . In this case, there is no separation of the wall boundary layer both upstream and downstream of the cylinder. Vortex separation from a circular cylinder near the wall was studied numerically in [13] based on the solution to the two-dimensional Navier–Stokes equations and Poisson equation for the pressure at  $80 < Re_d < 10^3$  and  $0.1 < \delta/d < 2.0$ . The main goal of research was the analysis of mech-

anisms for suppressing the vortex wake of the cylinder in the case of small gaps. It was found that vortex shedding regularity and fluctuation amplitude of the cylinder lifting force decrease with a decrease in the gap and/or Reynolds number. It was also shown that the mechanism for suppressing the vortex wake behind the cylinder is based on interaction between the shear layer behind the cylinder surface closest to the wall and shear layer on the wall with different-sign vorticities. The gap corresponding to suppression of the vortex wake decreased with increasing Reynolds number. In addition, regularity of a change in the frequency of vortex formation behind the cylinder with an approach to the wall was derived in the same work. In [14], dynamics of the turbulent wake and turbulence characteristics in the wake of a circular cylinder located near the wall were studied by Large Eddy Simulation (LES) based on the solution to three-dimensional non-stationary Navier–Stokes equations for incompressible fluid at  $Re_d = 1440$ . As a result, data on nonlinear interaction of the shear layer formed behind the cylinder and boundary layer on the wall were obtained depending on the size of a gap between the cylinder and wall. It was shown that at a small gap size, the flow stagnation point on the cylinder shifts towards the wall, the flow separation region on the cylinder increases, and significant change in the vortex trajectory is observed. There was also a delay in shear layer instability and formation of a wavy structure spanwise the cylinder, which then became three-dimensional and collapsed at the end of the recirculation area. When the cylinder was located beyond the wall boundary layer, the mutual effect of the shear layer on the cylinder and boundary layer on the wall weakened considerably, but the coherent structures behind the cylinder and small-scale eddies generated on their background have an influence on the laminar-turbulent transition on the wall.

Thus, the known investigations of the flow around a near-wall cylinder include mainly the data on the influence of a gap between the cylinder and wall on the frequency of vortex formation (the Karman wake), as well as information on interaction between the shear layers on the cylinder surface and on the wall, depending on gap and Reynolds number. Most of research has been performed for the turbulent flow regime. Meanwhile, it is known that at transverse streamlining of cylinder by an unbounded laminar flow at Reynolds number variations from 150 to 300, the transition to turbulent flow regime in a vortex wake is observed [15].

There are two points of view on the cause and mechanism of the laminar-turbulent transition when the critical Reynolds numbers are achieved ( $Re_d > 1.5 \cdot 10^5$ ) [15]. According to the first point of view, in the frontal part of the cylinder, a laminar boundary layer separates, then, it reattaches, and a laminar separation bubble is formed. Then, the attached boundary layer goes into a turbulent state and separates at the angular coordinate of approximately  $140^\circ$ . According to the second point of view, when approaching the critical Reynolds number, the laminar-turbulent transition occurs in the boundary layer on the cylinder surface, followed by a displacement of the separation point to the angular coordinate of  $140^\circ$  without the formation of a laminar separation bubble. In both cases, it is assumed that for the subcritical Reynolds numbers, the laminar boundary layer separates from the cylinder surface, and subsequent transition to the turbulent regime in the wake is possible (depending on the Reynolds number).

It is noted that in the range  $Re_d = 150\text{--}300$  in the region of vortex formation behind the cylinder at transition to the turbulent flow, the wake structure becomes three-dimensional. However, the transition processes in the wake, when the cylinder is located near the wall, including cylinder flow in the channel, have been studied insufficiently. The transient processes in the wake of transverse cylinder in a rectangular channel at  $10 < Re_d < 390$  were simulated numerically in [16]. The cylinder was located symmetrically relative to the channel walls, the blockage ratio (the ratio of the cylinder diameter to the channel height) was 0.2, and the aspect ratio (the ratio of cylinder length to its diameter) was about 10. It was shown that for  $Re_d < 180$ , the flow remains two-dimensional. At  $Re_d \geq 210$ , the three-dimensional effects were observed in the wake of the cylinder, caused by development of unstable plane flow

in the wake. When studying the flow around a transverse obstacle in a channel, it is important to understand the effect of the channel sidewalls on the flow in the wake of an obstacle at transient Reynolds numbers. Thus, in the case of a flow around a spanwise semi-cylindrical rib on the channel wall, the process of transition to turbulence in the mixing layer behind the rib is largely determined by the spiral motion of fluid from the channel sidewalls to its symmetry plane [17, 18]. It is unclear whether such motion exists behind the transverse circular cylinder when it is located near the channel wall. Moreover, many questions concerning the mechanism of transition to turbulence in the wake of the cylinder, for this case of flow separation, remain unexplored.

In this paper, we present the results of experimental studies of the flow structure in the wake of a transversely streamlined cylinder located near the wall of a rectangular channel in the range of Reynolds number  $Re_d = 125-250$ , where the signs of a transition to turbulence in the wake of the cylinder are observed. The process of vortex formation is analyzed, some features of flow structure evolution are revealed.

### 1. Experimental equipment and methods of research

The test section of experimental setup was a rectangular channel with width  $B = 50$  mm and height  $H = 20$  mm with light-transparent polycarbonate walls (Fig. 1). The channel is equipped with a smooth inlet, shaped according to the Bernoulli lemniscate. The length of the channel was  $L = 250$  mm. The choice of the cross-sectional dimensions of the channel was caused by the necessity to obtain the laminar flow in the channel within investigated range of Reynolds number  $Re_{D_h} = 1280-2600$ , calculated by hydraulic diameter of the channel  $D_h$ . In addition, the blockage ratio should not exceed the values accepted in such experiments ( $d/H \leq 0.15$ ), and cylinder aspect ratio  $B/d$  should be at least 10. The air flow rate in setup line was supported by the vacuum pumps and kept constant for one measurement regime using a set of critical nozzles located downstream of the test section. The error in flow rate maintaining did not exceed 0.25%.

A circular cylinder with diameter  $d = 3$  mm was mounted across the test section parallel to its wide wall at distance  $l = 100$  mm from the inlet cross section. This distance was chosen to locate this cylinder within the thickness of a boundary layer, developing on the channel wall, in the studied range of Reynolds numbers. In addition, the research tasks included revelation of spiral fluid movements from the channel sidewalls to its symmetry plane, if there is a gap between the obstacle (cylinder) and channel wall. As it was already mentioned, these movements were detected, when the spanwise rib was located on the channel wall [17]. Therefore, in the present case, the cylinder was located at the same distance from the inlet cross section of the channel as the rib in previous studies [17]. The distance from the cylinder axis to the nearest wall of the section was equal to cylinder diameter  $d$ , which corresponds to the 1.5 mm gap between the cylinder surface and channel wall. The studies were carried out for four values of the average flow velocity in the channel:  $U_0 = 0.65, 0.81, 1.13, \text{ and } 1.33$  m/s, and the following Reynolds numbers calculated by cylinder diameter ( $Re_d = U_0 d / \nu = 135, 167, 233, \text{ and } 276$ ) corresponded to these velocities. Here,  $\nu = 2 \cdot 10^{-5}$  is the kinematic viscosity of the working me-

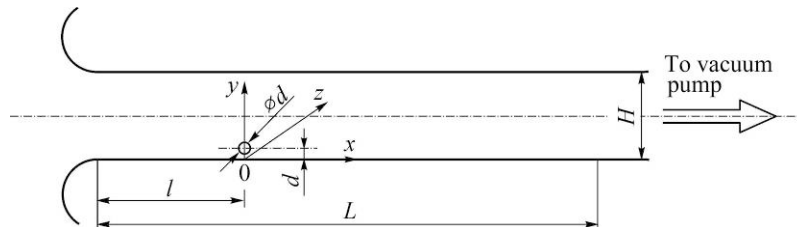


Fig. 1. Test section of experimental setup.

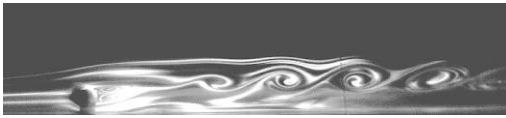


Fig. 2. Loss of shear layer stability and formation of vortices behind the cylinder at  $Re_d = 167$ .

View in channel symmetry plane  $xOy$ .

dium (air). In the studied range of Reynolds numbers, the boundary layer thickness in the region of cylinder installation varied approximately from 5.4 to 3.7 mm, i.e., a gap between the cylinder and channel wall for all values of Reynolds number remained less than the boundary layer thickness.

The experiments included visualization of the flow around the cylinder and measurement of dynamics of instantaneous vector fields of the flow velocity in its wake. To visualize the flow, the method of smoking wire was used. The smoke was generated with the help of nichrome wires located near the generatrix of the smooth inlet into the test section of setup. Oil was applied on the wire, and it evaporated, when electric current passed through the wire, creating a narrow concentrated smoke train. The flow pattern was registered in the light sheet plane by a high-speed monochrome video camera Fastec HiSpec. The visualization was carried out in the  $xOy$  plane (plane of channel symmetry) and in the plane parallel to  $xOz$ , at  $y = 4.5$  mm (tangent to the cylinder generatrix). The light sheet was created by a continuous-wave laser KLM-532/5000.

The instantaneous vector fields of the flow velocity in the cylinder wake and their dynamics are obtained using the SIV (Smoke Image Velocimetry) method [19]. The method is based on measuring the movements of turbulent structures for a fixed time interval between the frames of digital video registration of the flow pattern. The video was made, as in the case of flow visualization, by a high-speed monochrome Fastec HiSpec video camera in the light sheet plane. When carrying out the SIV measurements, special tracers (suspended small glycerin drops with the diameter of 1 to 5  $\mu\text{m}$ ) were seeded into the flow. The tracers were made by the FOG 2010 Plus aerosol generator. The operation of generator can introduce perturbations into the flow at test section inlet; to exclude this effect, a special accumulator was placed in front of the test section of setup; it was filled with aerosol before each experiment. During the experiment, the aerosol generator was switched off.

## 2. Results and discussion

The results of flow visualization and data on distribution of statistical characteristics of the flow in the cylinder wake, obtained from SIV measurements, showed the following. At Reynolds number  $Re_d = 135$ , the formation of vortex structures behind the cylinder is not observed. The spectra of flow velocity fluctuation measured in the plane of channel symmetry at distance  $x/d = 3.3, 4.3, 5.3$ , and  $6.7$  from the cylinder axis at  $y/d = 0.5$  and  $1.5$ , did not reveal the signs of regular vortex formation. At  $Re_d = 167$ , a closed laminar separation region consisting of two stationary symmetrical vortices is formed immediately behind the cylinder. Formation of a street of regular large-scale vortex structures is observed downstream of this region (Fig. 2). Due to the jet flow in the gap between the cylinder and channel wall, the flow around the cylinder is asymmetric, the symmetry plane of the laminar recirculation region immediately behind the cylinder is inclined to the wall at some angle. The jet flow does not allow vortex shedding from the lower (near the wall) surface of the cylinder, and the regular vortex structures are shed only from the upper (far from the wall) surface of the cylinder. Their formation starts at the distance of 5.5–6.5 cylinder diameters and, apparently, it is a consequence of stability loss by the shear layer behind the cylinder.

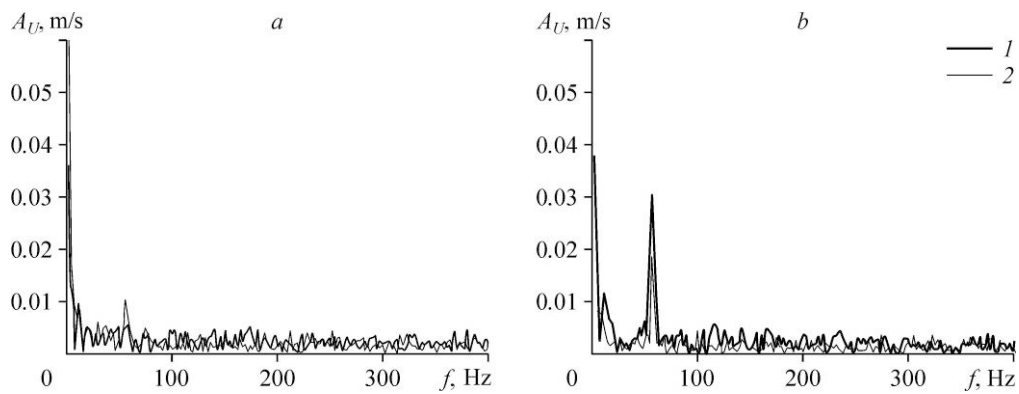


Fig. 3. Fluctuation spectra of streamwise velocity component of the flow behind the cylinder at distances  $x/d = 3.3$  (a) and  $6.7$  (b) at  $Re_d = 167$ .  $y/d = 1.5$  (1),  $0.5$  (2).

Data of flow visualization are confirmed by the results of measuring the fluctuation spectrum of the streamwise component of flow velocity behind the cylinder (Fig. 3): at all distances from the cylinder, a maximum is observed in the spectrum at distances from the wall  $y/d = 0.5$  and  $y/d = 1.5$ , corresponding to dimensionless vortex shedding frequency  $Sh = 0.21$  (Fig. 3). With an increase in the distance from the cylinder, the maximum value increases.

In the regime corresponding to the beginning of stability loss by the shear layer and vortex formation, the flow in the wake behind the cylinder remains quasi-two-dimensional along the whole width of the channel, excluding the boundary layer region on its sidewalls. In the near wake, the flow is laminar and almost flat, and the vortices forming behind the cylinder retain their integrity along the channel width (Fig. 4).

With an increase in the Reynolds number, the flow pattern in the wake of the cylinder changes significantly. The separation region immediately behind the cylinder is no longer stationary, and it is not possible to distinguish two symmetrical vortices in this region (Fig. 5). The separation region oscillates in the vertical plane. The vortex formation onset shifts upstream: the vortices are formed already at  $x/d \approx 3$ . Nevertheless, behind the cylinder, as at low Reynolds numbers, one street of vortices, separating from the upper generatrix of the cylinder, is formed. The size of these vortices increases with an increase in the Reynolds number, and distance from the wall, where they move, increases.

In the spectra of flow velocity fluctuations at all distances from the cylinder, one peak of fluctuations is observed at the vortex shedding frequency, and the second maximum is observed at multiple harmonic with  $y/d = 1.5$  (Fig. 6). Analysis of flow visualization data and oscillograms of the flow velocity indicates that appearance of the second maximum is caused by the difference between velocity fluctuations at the vortex shedding frequency and the harmonic law. The dimensionless vortex shedding frequency from the cylinder varies slightly with an increase in the Reynolds number: at  $Re_d = 233$ , it is  $Sh = 0.23$ , and at  $Re_d = 276$ ,

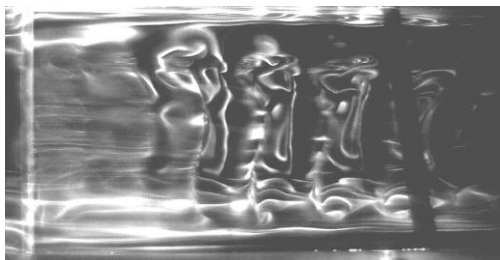


Fig. 4. Visualization of the flow in the wake of the cylinder in plane  $xOz$  at distance  $y/d = 1.5$  at  $Re_d = 167$ .

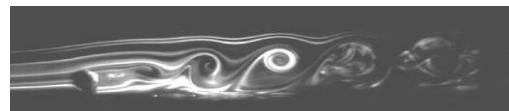


Fig. 5. Formation of vortices behind the cylinder at  $Re_d = 233$ . View in channel symmetry plane  $xOy$ .

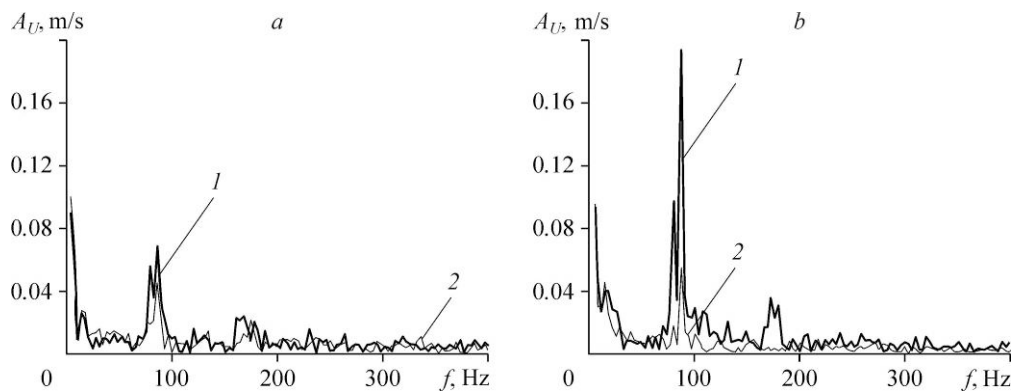


Fig. 6. Fluctuation spectra of streamwise velocity component of the flow behind the cylinder at  $Re_d = 233$ .

See nomenclature in Fig. 3.

it is  $Sh = 0.22$ . At  $Re_d = 233$ , there are the pronounced signs of three-dimensional flow in the wake of the cylinder (Fig. 7): vortices, formed behind the cylinder are split into several vortex bunches, when moving downstream.

It should be noted that throughout the investigated range of Reynolds numbers, no spiral movements of fluid from the channel side walls to its symmetry plane have been detected behind a cylinder near the wall. As was mentioned above, this plays a decisive role in the processes of transition to turbulence, when the flow is separated behind an obstacle located on the channel wall [17, 18]. In the studied flow, the transition to turbulence in the wake of the cylinder near the channel wall occurs at  $Re_d = 135$ – $276$  due to the loss of stability by the mixing layer.

Evolution of flow characteristics in the channel behind the cylinder can be judged by the changes in the profiles of flow velocity (Fig. 8) and its rms fluctuations at different distances from the cylinder with increasing Reynolds number (Fig. 9). The profiles were obtained from SIV-measurements with time averaging of 1000 instantaneous values of the flow velocity at each point. In the figures, the cylinder axis corresponds to coordinate  $y/d = 1.0$ .

According to information presented, in the area of a wake behind the cylinder, there is a velocity defect, which is smoothed (smeared out) with a distance from the cylinder. In addition, near the wall within the jet area, formed in a gap between the cylinder and channel wall, the maximal velocity is observed. With a distance from the cylinder, the distance from the wall both to the point of velocity minimum and maximum increases. However, the character of a change in the velocity profiles with increasing Reynolds number at the same distance from the cylinder is nonmonotonic. Thus, at  $Re_d = 167$  (Fig. 8b), the magnitude of velocity defect is more pronounced than at  $Re_d = 233$  (Fig. 8c). In addition, at  $Re_d = 135$ , in the near-wall region, the flow is close to pre-separation (Fig. 8a): there is characteristic S-shape of the velocity profile near the wall. With an increase in the Reynolds number to  $Re_d = 167$ , the signs of flow pre-separation on the channel wall behind the cylinder almost

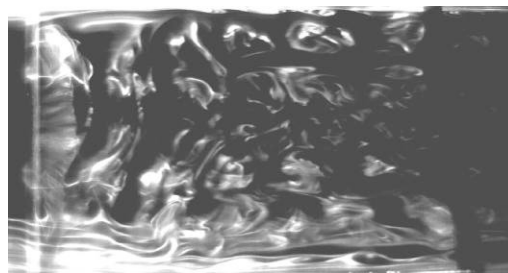


Fig. 7. Visualization of the flow in a wake of the cylinder in plane  $xOz$  at distance  $y/d = 1.5$  at  $Re_d = 233$ .

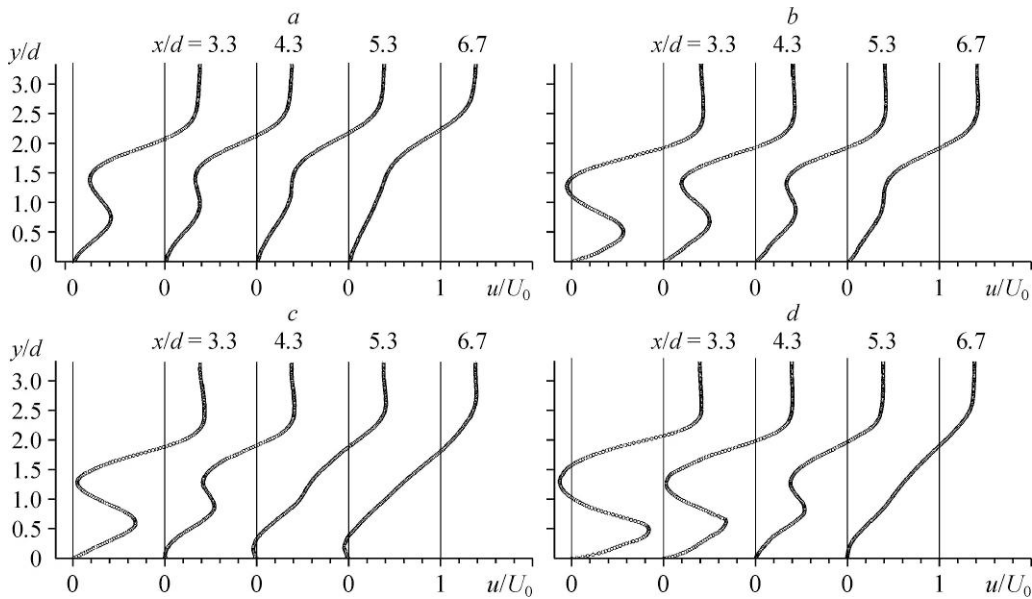


Fig. 8. Profiles of the flow velocity behind the cylinder in the plane of channel symmetry.  
 $Re_d = 135$  (a), 167 (b), 233 (c), 276 (d).

disappear (Fig. 8b), but at  $Re_d = 233$ , a separated flow is observed on the channel wall behind the cylinder: the flow velocity profiles at  $x/d \geq 4.3$  indicate the presence of reverse flows near the wall (Fig. 8c). With a further increase in  $Re_d$ , flow separation on the channel wall is not observed until  $x/d = 5.3$  (Fig. 8d).

The rms fluctuations of the streamwise component of flow velocity  $\sigma_u$  in the near wake of the cylinder (at  $x/d = 3.3$ ) have three pronounced local maxima along the transverse coordinate within the studied range of Reynolds numbers (Fig. 9). Their appearance relates, apparently, to interaction between the boundary of a jet formed in the gap between the cylinder and channel wall and shear layers formed, when the flow separates from the upper and lower surfaces of the cylinder. With a distance from the cylinder, the maxima closest to the wall are significantly smeared out. However, even here, as for the flow velocity profiles, with an increase in the Reynolds number, distributions of rms fluctuations of streamwise velocity component  $\sigma_u$  along the transverse coordinate at the same values of  $x/d$  vary nonmonotonically. Thus, at  $Re_d = 167$ , the maxima of  $\sigma_u$  for  $x/d = 4.3$  (Fig. 9b) are more pronounced than for  $Re_d = 135$  and 233 (Figs. 9a and 9c). Moreover, the maximum of  $\sigma_u$  closest to the wall at  $x/d = 3.3$  and 4.3 with an increase in the Reynolds number first moves away from the wall, then approaches it. The features of evolution of the profiles of streamwise flow velocity component and its rms fluctuations, observed in experiments in the range of Reynolds number  $Re_d = 135$ –267, are apparently caused by a loss of stability and transition to the turbulent flow regime in the wake of the cylinder and transition to the three-dimensional flow structure in the wake.

The influence of the channel side walls extends over a distance of not more than 10–15 % of the channel width and it is not important for a nonmonotonic change in the flow velocity profile in the wake of the cylinder and values of other flow parameters with increasing Reynolds number.



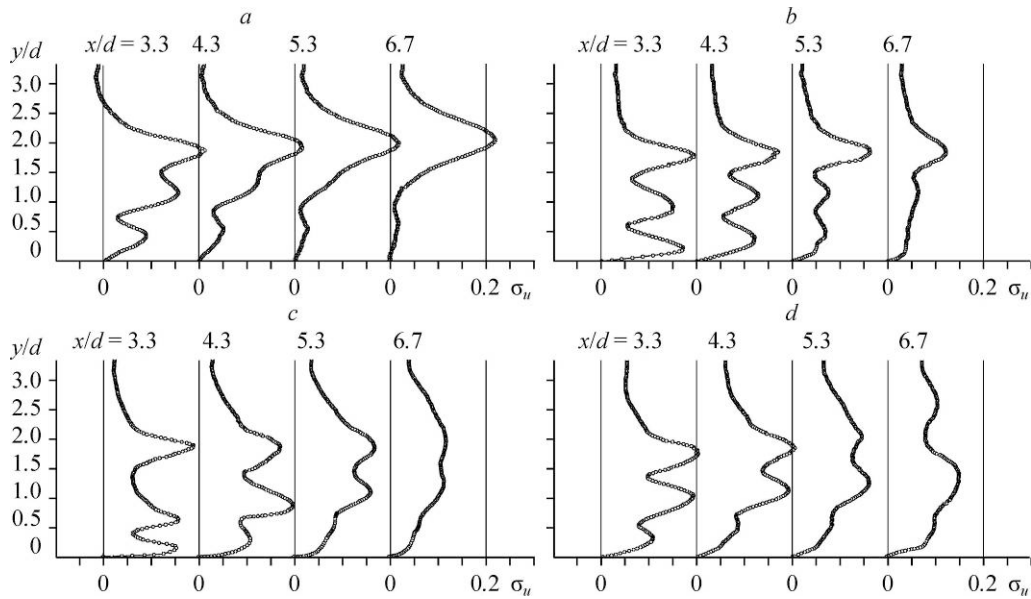


Fig. 9. Profiles of velocity fluctuations behind the cylinder in the plane of channel symmetry.  
 $Re_d = 135$  (a),  $167$  (b),  $233$  (c),  $276$  (d).

### Conclusion

Visual studies and measurements of instantaneous vector fields of the flow velocity in a wake of the cylinder mounted near the wall of a rectangular channel at distance  $y/d = 1$  from the wall were carried out. Based on the results of research, the following conclusions can be made.

1. In the range of Reynolds number  $Re_d = 135-276$ , a loss of stability of the shear layer in the wake of the cylinder and transition to the turbulent flow regime in the wake are observed.
2. At  $Re_d = 135-167$ , the stationary separation region with two symmetric closed vortices is formed immediately behind the cylinder. With increasing Reynolds number, the flow in this region becomes unstable, and this region oscillates in the vertical plane.
3. The large-scale regular vortices are formed only on the cylinder surface far from the channel wall. The jet flow in a gap between the cylinder and channel wall suppresses the formation of regular vortices on the cylinder surface nearby to the wall.
4. In contrast to the flow around a spanwise rib located on the channel wall, in the case of cross flow around the cylinder near the wall, spiral motion of fluid from the side walls of the channel to its symmetry plane is not observed. The transition to the turbulent flow behind the cylinder occurs due to the loss of stability by the shear layer, and the flow structure in the wake becomes essentially three-dimensional.
5. The laminar-turbulent transition in the wake of the cylinder with an increase in the Reynolds number in the studied range is accompanied by an upstream shift of the large-scale vortex formation onset.
6. In the transition to turbulence and three-dimensional flow pattern in the wake of the cylinder, a nonmonotonic change in the velocity profiles and its turbulent fluctuations is observed with an increase in the Reynolds number for the identical values of dimensionless distance downstream of the cylinder.

## References

1. **H. Schlichting**, *Boundary Layer Theory*, McGraw-Hill, New York, 1955.
2. **S.M. Belotserkovskii, V.N. Kotovskii, M.I. Nisht, and R.M. Fedorov**, Modeling the separation flow around a cylinder near a screen, *J. Eng. Phys. Thermophys.*, 1986, Vol. 50, No. 2, P. 129–134.
3. **L. Bearman and K.M. Zdravkovich**, Flow around a circular cylinder near a plane boundary, *J. Fluid Mech.*, 1978, Vol. 89, pt. 1, P. 33–47.
4. **A.B. Ezerskii**, Pressure pulsations on a rigid wall caused by a vortex street, *Fluid Dynamics*, 1986, Vol. 21, No. 2, P. 311–313.
5. **F. Angrilli, S. Bergamaschi, and V. Cossalter**, Investigation of wall induced modifications to vortex shedding from a circular cylinder, *J. Fluid Eng.*, 1982, Vol. 104, No. 4, P. 518–522.
6. **T. Marumo, K. Suzuki, and T. Sato**, Turbulent heat transfer in a flat plate boundary layer disturbed by a cylinder, *Int. J. Heat Fluid Flow*, 1985, Vol. 6, No. 4, P. 241–248.
7. **H. Suzuki, K. Suzuki, and T. Sato**, Dissimilarity between heat and momentum transfer in a turbulent boundary layer disturbed by a cylinder, *Int. J. Heat Mass Transfer*, 1988, Vol. 31, No. 2, P. 259–265.
8. **V.M. Molochnikov, N.I. Mikheev, I.A. Davletshin, and R.E. Faskhutdinov**, Dynamics of transfer of turbulent pulsations of hydrodynamic and thermal parameters in a wake behind a transverse cylinder near the wall, *Izv. RAN. Energetika*, 2007, No. 6, P. 80–86.
9. **N.D. Dikovskaya**, Experimental and numerical study of transverse streamlining of a cylinder near a flat screen, Ph.D Thesis, Novosibirsk, 1990.
10. **I. Khabbouchi, M.S. Guellouz, and S.B. Nasrallah**, A study of the effect of the jet-like flow on the near wake behind a circular cylinder close to a plane wall, *Exp. Therm. and Fluid Sci.*, 2013, No. 44, P. 285–300.
11. **A.A. Oner, M.S. Kirkgoz, and M.S. Akoz**, Interaction of a current with a circular cylinder near a rigid bed, *Ocean Engng.*, 2008, No. 35, P. 1492–1504.
12. **S.J. Price, D. Summer, J.G. Smith, K. Leong, and M.P. Paidoussis**, Flow visualization around a circular cylinder near to a plane wall, *J. Fluids and Structures*, 2002, Vol. 16, No. 2, P. 175–191.
13. **C. Lei, L. Cheng, S.W. Armfield, and K. Kavanagh**, Vortex shedding suppression for flow over a circular cylinder near a plane boundary, *Ocean Engng.*, 2000, No. 27, P. 1109–1127.
14. **S. Sarkar and S. Sarkar**, Vortex dynamics of a cylinder wake in proximity to a wall, *J. Fluids and Structures*, 2010, Vol. 26, No. 1, P. 19–40.
15. **A.A. Zhukauskas**, *Convective Transfer in Heat Exchangers*, Nauka, Moscow, 1982.
16. **N. Kanaris, D. Grigoriadis, and S. Kassinos**, Three dimensional flow around a circular cylinder confined in a plane channel, *Phys. Fluids*, 2011, Vol. 23, No. 1, P. 1–14.
17. **V.M. Molochnikov, A.B. Mazo, A.V. Malyukov, E.I. Kalinin, N.I. Mikheev, O.A. Dushina, and A.A. Paereliy**, Distinctive features of vertical structures generation in separated channel flow behind a rib under transition to turbulence, *Thermophysics and Aeromechanics*, 2014, Vol. 21, No. 3, P. 309–317.
18. **A.B. Mazo and D.I. Okhotnikov**, Local transition to turbulence behind an obstacle for a nominally laminar flow, *Lobachevskii J. Mathematics*, 2016, P. 360–367.
19. **N.I. Mikheev and N.S. Dushin**, A method for measuring the dynamics of velocity vector fields in a turbulent flow using smoke image-visualization videos, *Instruments and Experimental Techniques*, 2016, No. 6, P. 882–889.